# Sketch-Based Streaming Anomaly Detection in Dynamic Graphs

**Siddharth Bhatia**
National University of Singapore
siddharth@comp.nus.edu.sg

**Mohit Wadhwa**
mailmohitwadhwa@gmail.com

**Philip S. Yu**
University of Illinois at Chicago
psyu@uic.edu

**Bryan Hooi**
National University of Singapore
bhooi@comp.nus.edu.sg

## Abstract

Given a stream of graph edges from a dynamic graph, how can we assign anomaly scores to edges and subgraphs in an online manner, for the purpose of detecting unusual behavior, using constant time and memory? For example, in intrusion detection, existing work seeks to detect either anomalous edges or anomalous subgraphs, but not both. In this paper, we first extend the count-min sketch data structure to a higher-order sketch. This higher-order sketch has the useful property of preserving the dense subgraph structure (dense subgraphs in the input turn into dense submatrices in the data structure). We then propose four online algorithms that utilize this enhanced data structure, which (a) detect both edge and graph anomalies; (b) process each edge and graph in constant memory and constant update time per newly arriving edge, and; (c) outperform state-of-the-art baselines on four real-world datasets. Our method is the first streaming approach that incorporates dense subgraph search to detect graph anomalies in constant memory and time.

## 1 Introduction

Consider an intrusion detection system, in which many forms of anomalous behavior can be described as a group of attackers making a large number of connections to some set of targeted machines to restrict accessibility or look for potential vulnerabilities. We can model this as a dynamic graph, where nodes correspond to machines, and each edge represents a timestamped connection from one machine to another. In this graph, anomalous behavior often takes the form of a dense subgraph, as shown in several real-world datasets in [1–3]. Thus, we ask the question: Given a stream of graph edges from a dynamic graph, how can we assign anomaly scores to both edges and subgraphs in an online manner, for the purpose of detecting unusual behavior, using constant memory and constant update time per newly arriving edge?

Several approaches [4–10] aim to detect anomalies in graph settings. However, these approaches focus on static graphs, whereas many real-world graphs are time-evolving in nature. In streaming or online graph scenarios, some methods can detect the presence of anomalous edges, [3, 11–13], while others can detect anomalous subgraphs [1, 2, 14]. However, all existing methods are limited to either anomalous edge or graph detection but not able to detect both kinds of anomalies, as summarized in Table 1. As we discuss in Section 7, our approach outperforms existing methods in both accuracy and running time; and on both anomalous edge and subgraph detection scenarios. Moreover, our approach is the only streaming method that makes use of dense subgraph search to detect graph anomalies while only requiring constant memory and time.

Table 1: Comparison of relevant anomaly detection approaches.

| Property | DenseStream (KDD'17) | SedanSpot (ICDM'20) | MIDAS-R (AAAI'20) | PENminer (KDD'20) | F-FADE (WSDM'21) | DenseAlert (KDD'17) | SpotLight (KDD'18) | AnomRank (KDD'19) | **Our Method** (2021) |
|---|---|---|---|---|---|---|---|---|---|
| **Edge Anomaly** | ✓ | ✓ | ✓ | ✓ | ✓ | – | – | – | ✓ |
| **Graph Anomaly** | – | – | – | – | – | ✓ | ✓ | ✓ | ✓ |
| **Constant Memory** | – | ✓ | ✓ | – | ✓ | – | ✓ | – | ✓ |
| **Constant Update Time** | – | ✓ | ✓ | ✓ | ✓ | – | ✓ | – | ✓ |
| **Dense Subgraph Search** | ✓ | – | – | – | – | ✓ | – | – | ✓ |

We first extend the two-dimensional sketch to a *higher-order sketch* to enable it to embed the relation between the source and destination nodes in a graph. A higher-order sketch has the useful property of preserving the dense subgraph structure; dense subgraphs in the input turn into dense submatrices in this data structure. Thus, the problem of detecting a dense subgraph from a large graph reduces to finding a dense submatrix in a constant size matrix, which can be achieved in constant time. The higher-order sketch allows us to propose several algorithms to detect both anomalous edges and subgraphs in a streaming manner. We introduce two edge anomaly detection methods, ANOEDGE-G, and ANOEDGE-L, and two graph anomaly detection methods ANOGRAPH, and ANOGRAPH-K, that use the same data structure to detect the presence of a dense submatrix, and consequently anomalous edges, or subgraphs respectively. All our approaches process edges and graphs in constant time, and are independent of the graph size, i.e., they require constant memory. We also provide theoretical guarantees on the higher-order sketch estimate and the submatrix density measure. In summary, the main contributions of our paper are:

1. **Higher-Order Sketch (Section 4)**: We transform the dense subgraph detection problem into finding a dense submatrix (which can be achieved in constant time) by extending the count-min sketch (CMS) [15] data structure to a higher-order sketch.

2. **Streaming Anomaly Detection (Sections 5,6)**: We propose four novel online approaches to detect anomalous edges and graphs in real-time, with constant memory and update time. Moreover, this is the first streaming work that incorporates dense subgraph search to detect graph anomalies in constant memory/time.

3. **Effectiveness (Section 7)**: We outperform all state-of-the-art streaming edge and graph anomaly detection methods on four real-world datasets.

**Reproducibility**: Our code and datasets are available at https://github.com/Stream-AD/AnoGraph.

## 2    Related Work

Our work is closely related to areas like anomaly detection on graphs [16–23] and streams [24–32], and streaming algorithms [33–37]. Higher-order sketches are discussed in [37], however, they are restricted to count-sketches and non-graph settings. [38, 39] discuss deep learning based anomaly detection, however, such approaches are unable to detect anomalies in a streaming manner. [4–10] are limited to anomaly detection in static graphs. In this section, however, we limit our review only to methods detecting edge and graph anomalies in dynamic graphs; see [40] for an extensive survey.

**Edge Stream Methods:** HOTSPOT [41] detects nodes whose egonets suddenly change. RHSS [42] focuses on sparsely-connected graph parts. CAD [43] localizes anomalous changes using commute time distance measurement. More recently, DENSESTREAM [1] maintains and updates a dense subtensor in a tensor stream. SEDANSPOT [11] identifies edge anomalies based on edge occurrence, preferential attachment, and mutual neighbors. PENminer [12] explores the persistence of activity snippets, i.e., the length and regularity of edge-update sequences' reoccurrences. F-FADE [13] aims to detect anomalous interaction patterns by factorizing their frequency. MIDAS [3] identifies microcluster-based anomalies. However, all these methods are unable to detect graph anomalies.

**Graph Stream Methods:** DTA/STA [44] approximates the adjacency matrix of the current snapshot using matrix factorization. COPYCATCH [45] spots near-bipartite cores where each node is connected to others in the same core densely within a short time. SPOT/DSPOT [30] use extreme value theory to automatically set thresholds for anomalies. IncGM+ [46] utilizes incremental method to process graph updates. More recently, DENSEALERT identifies subtensors created within a short time and utilizes incremental method to process graph updates or subgraphs more efficiently. SPOTLIGHT

[2] discovers anomalous graphs with dense bi-cliques, but uses a randomized approach without any search for dense subgraphs. ANOMRANK [14], inspired by PageRank [47], iteratively updates two score vectors and computes anomaly scores. However, these methods are slow and do not detect edge anomalies. Moreover, they do not search for dense subgraphs in constant memory and time.

## 3 Problem

Let $\mathscr{E} = \{e_1, e_2, \cdots\}$ be a stream of weighted edges from a time-evolving graph $\mathcal{G}$. Each arriving edge is a tuple $e_i = (u_i, v_i, w_i, t_i)$ consisting of a source node $u_i \in \mathcal{V}$, a destination node $v_i \in \mathcal{V}$, a weight $w_i$, and a time of occurrence $t_i$, the time at which the edge is added to the graph. For example, in a network traffic stream, an edge $e_i$ could represent a connection made from a source IP address $u_i$ to a destination IP address $v_i$ at time $t_i$. We do not assume that the set of vertices $\mathcal{V}$ is known a priori: for example, new IP addresses or user IDs may be created over the course of the stream.

We model $\mathcal{G}$ as a directed graph. Undirected graphs can be handled by treating an incoming undirected edge as two simultaneous directed edges, one in each direction. We also allow $\mathcal{G}$ to be a multigraph: edges can be created multiple times between the same pair of nodes. Edges are allowed to arrive simultaneously: i.e. $t_{i+1} \geq t_i$, since in many applications $t_i$ is given as a discrete time tick.

The desired properties of our algorithm are as follows:

- **Detecting Anomalous Edges:** To detect whether the edge is part of an anomalous subgraph in an online manner. Being able to detect anomalies at the finer granularity of edges allows early detection so that recovery can be started as soon as possible and the effect of malicious activities is minimized.
- **Detecting Anomalous Graphs:** To detect the presence of an unusual subgraph (consisting of edges received over a period of time) in an online manner, since such subgraphs often correspond to unexpected behavior, such as coordinated attacks.
- **Constant Memory and Update Time:** To ensure scalability, memory usage and update time should not grow with the number of nodes or the length of the stream. Thus, for a newly arriving edge, our algorithm should run in constant memory and update time.

## 4 Higher-Order Sketch & Notations

Count-min sketches (CMS) [15] are popular streaming data structures used by several online algorithms [48]. CMS uses multiple hash functions to map events to frequencies, but unlike a hash table uses only sub-linear space, at the expense of overcounting some events due to collisions. Frequency is approximated as the minimum over all hash functions. CMS, shown in Figure 1(a), is represented as a two-dimensional matrix where each row corresponds to a hash function and hashes to the same number of buckets (columns).

We introduce a Higher-order CMS (H-CMS) data structure where each hash function maps multi-dimensional input to a generic tensor instead of mapping it to a row vector. H-CMS enhances CMS by separately hashing the individual components of an entity thereby maintaining more information. Figure 1(b) shows a 3-dimensional H-CMS that can be used to hash two-dimensional entities such as graph edges to a matrix. The source node is hashed to the first dimension and the destination node to the other dimension of the sketch matrix, as opposed to the original CMS that will hash the entire edge to a one-dimensional row vector as shown in Figure 1(a).

**Theorem 1.** *(Proof in Appendix C) H-CMS has the same estimate guarantees as the original CMS.*

We use a 3-dimensional H-CMS (operations described in Appendix A) where the number of hash functions is denoted by $n_r$, and matrix $\mathcal{M}$ corresponding to each hash function is of dimension $n_b \times n_b$, i.e., a square matrix. A hash function denoted by $h(u)$ maps an entity $u$ to an integer in the range $[0, n_b)$. A 3-dimensional H-CMS maps edge $(u, v)$ to a matrix index $(h(u), h(v))$, i.e. the source node is mapped to a row index and the destination node is mapped to a column index. Therefore, each matrix in a 3-dimensional H-CMS captures the essence of a graph adjacency matrix. Dense subgraph detection can thus be transformed into a dense submatrix detection problem (as shown in Figure 2) where the size of the matrix is a small constant, independent of the number of edges or the graph size.
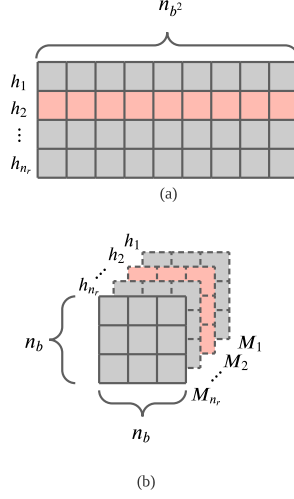
3

Figure 1: (a) Original CMS (b) Higher-order CMS
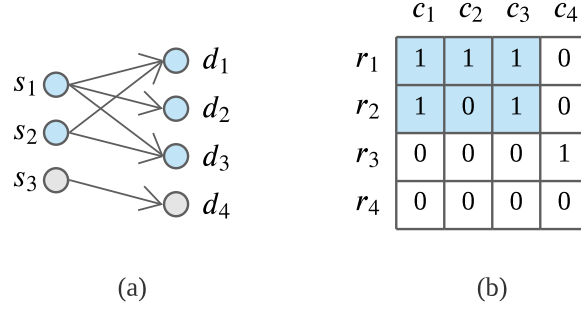


(a)                                    (b)

Figure 2: (a) Dense subgraph in the original graph between source nodes $s_1, s_2$, and destination nodes $d_1, d_2, d_3$ is transformed to a (b) Dense submatrix between rows $r_1, r_2$, and columns $c_1, c_2, c_3$ in the H-CMS.

Frequently used symbols are discussed in Table 2, and we leverage the subgraph density measure discussed in [49] to define the submatrix $(S_x, T_x)$ density.

**Definition 1.** *Given matrix $\mathcal{M}$, density of a submatrix of $\mathcal{M}$ represented by $S_x \subseteq S$ and $T_x \subseteq T$, is:*

$$\mathcal{D}(\mathcal{M}, S_x, T_x) = \frac{\sum_{s \in S_x} \sum_{t \in T_x} \mathcal{M}[s][t]}{\sqrt{|S_x||T_x|}} \tag{1}$$

## 5 Edge Anomalies

In this section, using the H-CMS data structure, we propose ANOEDGE-G and ANOEDGE-L to detect edge anomalies by checking whether the received edge when mapped to a sketch matrix element is part of a dense submatrix. ANOEDGE-G finds a **G**lobal dense submatrix and performs well in practice while ANOEDGE-L maintains and updates a **L**ocal dense submatrix around the matrix element and therefore has better time complexity.

### 5.1 ANOEDGE-G

ANOEDGE-G, as described in Algorithm 1, maintains a *temporally decaying* H-CMS, i.e. whenever 1 unit of time passes, we multiply all the H-CMS counts by a fixed factor $\alpha$ (lines 2,4). This decay

Table 2: Table of symbols.

| Symbol | Definition |
|---|---|
| $n_r$ | number of hash functions |
| $n_b$ | number of buckets |
| $h(u)$ | hash function $u \rightarrow [0, n_b)$ |
| $\mathcal{M}$ | a square matrix of dimensions $n_b \times n_b$ |
| $\mathcal{M}[i][j]$ | element at row index i and column index j |
| $S$ | set of all row indices |
| $S_{cur}$ | set of current submatrix row indices |
| $S_{rem}$ | set of remaining row indices i.e. indices not part of current submatrix |
| $T$ | set of all column indices |
| $T_{cur}$ | set of current submatrix column indices |
| $T_{rem}$ | set of remaining column indices i.e. indices not part of current submatrix |
| $[z]$ | set of all integers in the range $[1, z]$, i.e., $\{1, 2, ..., z\}$ |
| $\mathcal{D}(\mathcal{M}, S_x, T_x)$ | density of submatrix $(S_x, T_x)$ |
| $\mathcal{E}(\mathcal{M}, S_x, T_x)$ | sum of elements of submatrix $(S_x, T_x)$ |
| $\mathcal{R}(\mathcal{M}, u, T_x)$ | submatrix row-sum i.e. sum of elements of submatrix $(\{u\}, T_x)$ |
| $\mathcal{C}(\mathcal{M}, S_x, v)$ | submatrix column-sum i.e. sum of elements of submatrix $(S_x, \{v\})$ |
| $\mathcal{L}(\mathcal{M}, u, v, S_x, T_x)$ | likelihood of index $(u, v)$ w.r.t. submatrix $(S_x, T_x)$ |
| $d_{max}$ | maximum reported submatrix density |

simulates the gradual 'forgetting' of older and hence more outdated information. When an edge $(u, v)$ arrives, $u, v$ are mapped to matrix indices $h(u)$, $h(v)$ respectively for each hash function $h$, and the corresponding H-CMS counts are updated (line 5). EDGE-SUBMATRIX-DENSITY procedure (described below) is then called to compute the density of a dense submatrix around $(h(u), h(v))$. Density is reported as the anomaly score for the edge; a larger density implies that the edge is more likely to be anomalous.

EDGE-SUBMATRIX-DENSITY procedure calculates the density of a dense submatrix around a given index $(u, v)$. A $1 \times 1$ submatrix represented by $S_{cur}$ and $T_{cur}$, is initialized with row-index $u$ and column index $v$ (line 9). The submatrix is iteratively expanded by greedily selecting a row $u_p$ from $S_{rem}$ (or a column $v_p$ from $T_{rem}$) that obtains the maximum row (or column) sum with the current submatrix (lines 14,16). This selected row $u_p$ (or column $v_p$) is removed from $S_{rem}$ (or $T_{rem}$), and added to $S_{cur}$ (or $T_{cur}$) (lines 15,17). The process is repeated until both $S_{rem}$ and $T_{rem}$ are empty (line 11). Density of the current submatrix is computed at each iteration of the submatrix expansion process and the maximum over all greedily formed submatrix densities is returned (line 18).

**Proposition 1.** *(Proof in Appendix D.1) Time complexity of Algorithm 1 is $O(|\mathscr{E}| * n_r * n_b^2)$* [1].

**Proposition 2.** *(Proof in Appendix D.1) Memory complexity of Algorithm 1 is $O(n_r * n_b^2)$.*

### 5.2 ANOEDGE-L

Inspired by Definition 1, we define the likelihood measure of a matrix index $(u, v)$ with respect to a submatrix $(S_x, T_x)$, as the sum of the elements of submatrix $(S_x, T_x)$ that either share row with index $v$ or column with index $u$ divided by the total number of such elements.

**Definition 2.** *Given matrix $\mathcal{M}$, likelihood of an index $(u, v)$ with respect to a submatrix represented by $S_x \subseteq S$ and $T_x \subseteq T$, is:*

$$\mathcal{L}(\mathcal{M}, u, v, S_x, T_x) = \frac{\sum_{(s,t) \in S_x \times v \cup u \times T_x} \mathcal{M}[s][t]}{|S_x \times v \cup u \times T_x|} \tag{2}$$

ANOEDGE-L, as described in Algorithm 2, maintains a temporally decaying H-CMS to store the edge counts. We also initialize a mutable submatrix of size $1 \times 1$ with a random element, and represent

---

[1]This is for processing all edges; the time per edge is constant.

---

**Algorithm 1:** ANOEDGE-G : Streaming Anomaly Edge Scoring

---

**Input:** Stream $\mathscr{E}$ of edges over time
**Output:** Anomaly score per edge

**1 Procedure** ANOEDGE-G ($\mathscr{E}$)

  **2**    Initialize H-CMS matrix $\mathcal{M}$ for edge count        `// H-CMS data structure`

  **3**    **while** *new edge $e = (u, v, w, t) \in \mathscr{E}$ is received* **do**

  **4**        Temporal decay H-CMS with timestamp change        `// decay count`

  **5**        Update H-CMS matrix $\mathcal{M}$ for new edge $(u, v)$ with value $w$    `// update count`

  **6**        **output** $score(e) \leftarrow$ EDGE-SUBMATRIX-DENSITY$(\mathcal{M}, h(u), h(v))$

**7 Procedure** EDGE-SUBMATRIX-DENSITY ($\mathcal{M}, u, v$)

  **8**    $S \leftarrow [n_b];\ \ T \leftarrow [n_b];\ \ S_{cur} \leftarrow \{u\};\ \ T_{cur} \leftarrow \{v\};\ \ S_{rem} \leftarrow S/\{u\};\ \ T_{rem} \leftarrow T/\{v\}$

  **9**    $d_{max} \leftarrow \mathcal{D}(\mathcal{M}, S_{cur}, T_{cur})$

  **10**    **while** $S_{rem} \neq \emptyset\ \ \vee\ \ T_{rem} \neq \emptyset$ **do**

  **11**        $u_p \leftarrow \text{argmax}_{s_p \in S_{rem}}\ \mathcal{R}(\mathcal{M}, s_p, T_{cur})$      `// submatrix max row-sum index`

  **12**        $v_p \leftarrow \text{argmax}_{t_p \in T_{rem}}\ \mathcal{C}(\mathcal{M}, S_{cur}, t_p)$      `// submatrix max column-sum index`

  **13**        **if** $\mathcal{R}(\mathcal{M}, u_p, T_{cur}) > \mathcal{C}(\mathcal{M}, S_{cur}, v_p)$ **then**

  **14**            $S_{cur} \leftarrow S_{cur} \cup \{u_p\};\ \ S_{rem} \leftarrow S_{rem}/\{u_p\}$

  **15**        **else**

  **16**            $T_{cur} \leftarrow T_{cur} \cup \{v_p\};\ \ T_{rem} \leftarrow T_{rem}/\{v_p\}$

  **17**        $d_{max} \leftarrow max(d_{max}, \mathcal{D}(\mathcal{M}, S_{cur}, T_{cur}))$

  **18**    **return** $d_{max}$        `// dense submatrix density`

---

it as $(S_{cur}, T_{cur})$. As we process edges, we greedily update $(S_{cur}, T_{cur})$ to maintain it as a dense submatrix. When an edge arrives, H-CMS counts are first updated, and the received edge is then used to check whether to *expand* the current submatrix (line 7). If the submatrix density increases upon the addition of the row (or column), then the row-index $h(u)$ (or column-index $h(v)$) is added to the current submatrix, $(S_{cur}, T_{cur})$. To remove the row(s) and column(s) decayed over time, the process iteratively selects the row (or column) with the minimum row-sum (or column-sum) until removing it increases the current submatrix density. This ensures that the current submatrix is as *condensed* as possible (line 9). As defined in Definition 2, ANOEDGE-L computes the likelihood score of the edge with respect to $(S_{cur}, T_{cur})$ (line 10). A higher likelihood measure implies that the edge is more likely to be anomalous.

---

**Algorithm 2:** ANOEDGE-L : Streaming Anomaly Edge Scoring

---

**Input:** Stream $\mathscr{E}$ of edges over time
**Output:** Anomaly score per edge

**1 Procedure** ANOEDGE-L ($\mathscr{E}$)

  **2**    Initialize H-CMS matrix $\mathcal{M}$ for edges count        `// H-CMS data structure`

  **3**    Initialize a randomly picked $1 \times 1$ submatrix $(S_{cur}, T_{cur})$    `// mutable submatrix`

  **4**    **while** *new edge $e = (u, v, w, t) \in \mathscr{E}$ is received* **do**

  **5**        Temporal decay H-CMS with timestamp change        `// decay count`

  **6**        Update H-CMS matrix $\mathcal{M}$ for new edge $(u, v)$ with value $w$    `// update Count`

  **7**        ▷ **Check and Update Submatrix:**

  **8**        Expand $(S_{cur}, T_{cur})$        `// expand submatrix`

  **9**        Condense $(S_{cur}, T_{cur})$        `// condense submatrix`

  **10**        **output** $score(e) \leftarrow \mathcal{L}(\mathcal{M}, h(u), h(v), S_{cur}, T_{cur})$    `// from Definition 2`

---

**Proposition 3.** *(Proof in Appendix D.2) Time complexity of Algorithm 2 is* $O(n_r * n_b^2 + |\mathscr{E}| * n_r * n_b)$.

**Proposition 4.** *(Proof in Appendix D.2) Memory complexity of Algorithm 2 is* $O(n_r * n_b^2)$.

# 6 Graph Anomalies

We now propose ANOGRAPH and ANOGRAPH-K to detect graph anomalies by first mapping the graph to a higher-order sketch, and then checking for a dense submatrix. These are the first streaming algorithms that make use of dense subgraph search to detect graph anomalies in constant memory and time. ANOGRAPH greedily finds a dense submatrix with a 2-approximation guarantee on the density measure. ANOGRAPH-K leverages EDGE-SUBMATRIX-DENSITY from Algorithm 1 to greedily find a dense submatrix around $K$ strategically picked matrix elements performing equally well in practice.

## 6.1 ANOGRAPH

ANOGRAPH, as described in Algorithm 3, maintains an H-CMS to store the edge counts that are reset whenever a new graph arrives. The edges are first processed to update the H-CMS counts. ANOGRAPH-DENSITY procedure (described below) is then called to find the dense submatrix. ANOGRAPH reports anomaly score as the density of the detected (dense) submatrix; a larger density implies that the graph is more likely to be anomalous.

ANOGRAPH-DENSITY procedure computes the density of a dense submatrix of matrix $\mathcal{M}$. The current dense submatrix is initialised as matrix $\mathcal{M}$ and then the row (or column) from the current submatrix with minimum row (or column) sum is greedily removed. This process is repeated until $S_{cur}$ and $T_{cur}$ are empty (line 12). The density of the current submatrix is computed at each iteration of the submatrix expansion process and the maximum over all densities is returned (line 19).

Algorithm 3 is a special case of finding the densest subgraph in a directed graph problem [49] where the directed graph is represented as an adjacency matrix and detecting the densest subgraph essentially means detecting dense submatrix. We now provide a guarantee on the density measure.

**Theorem 2.** *(Proof in Appendix E.1) Algorithm 3 achieves a 2-approximation guarantee for the densest submatrix problem.*

---

**Algorithm 3:** ANOGRAPH: Streaming Anomaly Graph Scoring

**Input:** Stream $\mathscr{G}$ of edges over time
**Output:** Anomaly score per graph

1 **Procedure** ANOGRAPH ($\mathscr{G}$)
2      Initialize H-CMS matrix $\mathcal{M}$ for graph edges count      `// H-CMS data structure`
3      **while** *new graph $G \in \mathscr{G}$ is received* **do**
4          Reset H-CMS matrix $\mathcal{M}$ for graph $G$      `// reset count`
5          **for** *edge $e = (u, v, w, t) \in G$* **do**
6              Update H-CMS matrix $\mathcal{M}$ for edge $(u, v)$ with value $w$      `// update count`
7          **output** $score(G) \leftarrow$ ANOGRAPH-DENSITY($\mathcal{M}$)      `// anomaly score`

8 **Procedure** ANOGRAPH-DENSITY ($\mathcal{M}$)
9      $S_{cur} \leftarrow [n]$; $T_{cur} \leftarrow [n]$      `// initialize to size of` $\mathcal{M}$
10     $d_{max} \leftarrow \mathcal{D}(\mathcal{M}, S_{cur}, T_{cur})$
11     **while** $S_{cur} \neq \emptyset \ \lor \ T_{cur} \neq \emptyset$ **do**
12         $u_p \leftarrow \operatorname{argmin}_{s_p \in S_{cur}} \mathcal{R}(\mathcal{M}, s_p, T_{cur})$      `// submatrix min row-sum index`
13         $v_p \leftarrow \operatorname{argmin}_{t_p \in T_{cur}} \mathcal{C}(\mathcal{M}, S_{cur}, t_p)$      `// submatrix min column-sum index`
14         **if** $\mathcal{R}(\mathcal{M}, u_p, T_{cur}) < \mathcal{C}(\mathcal{M}, S_{cur}, v_p)$ **then**
15             $S_{cur} \leftarrow S_{cur}/\{u_p\}$      `// remove row`
16         **else**
17             $T_{cur} \leftarrow T_{cur}/\{v_p\}$      `// remove column`
18         $d_{max} \leftarrow max(d_{max}, \mathcal{D}(\mathcal{M}, S_{cur}, T_{cur}))$
19     **return** $d_{max}$      `// dense submatrix density`

---

**Proposition 5.** *(Proof in Appendix E.1) Time complexity of Algorithm 3 is $O(|\mathscr{G}| * n_r * n_b^2 + |\mathscr{E}| * n_r)$.*

**Proposition 6.** *(Proof in Appendix E.1) Memory complexity of Algorithm 3 is $O(n_r * n_b^2)$.*

## 6.2 ANOGRAPH-K

Similar to ANOGRAPH, ANOGRAPH-K maintains an H-CMS which is reset whenever a new graph arrives. It uses the ANOGRAPH-K-DENSITY procedure (described below) to find the dense submatrix. ANOGRAPH-K is summarised in Algorithm 4.

ANOGRAPH-K-DENSITY computes the density of a dense submatrix of matrix $\mathcal{M}$. The intuition comes from the heuristic that the matrix elements with a higher value are more likely to be part of a dense submatrix. Hence, the approach considers $K$ largest elements of the matrix $\mathcal{M}$ and calls EDGE-SUBMATRIX-DENSITY from Algorithm 1 to get the dense submatrix around each of those elements (line 14). The maximum density over the considered $K$ dense submatrices is returned.

---

**Algorithm 4:** ANOGRAPH-K: Streaming Anomaly Graph Scoring

**Input:** Stream $\mathscr{G}$ of edges over time
**Output:** Anomaly score per graph

1 **Procedure** ANOGRAPH-K ($\mathscr{G}, K$)
2    Initialize H-CMS matrix $\mathcal{M}$ for graph edges count     // H-CMS data structure
3    **while** *new graph $G \in \mathscr{G}$ is received* **do**
4       Reset H-CMS matrix $\mathcal{M}$ for graph $G$     // reset count
5       **for** *edge $e = (u, v, w, t) \in G$* **do**
6          Update H-CMS matrix $\mathcal{M}$ for edge $(u, v)$ with value $w$   // update count
7       **output** $score(G) \leftarrow$ ANOGRAPH-K-DENSITY($\mathcal{M}, K$)     // anomaly score

8 **Procedure** ANOGRAPH-K-Density ($\mathcal{M}, K$)
9    $B \leftarrow [n] \times [n]$     // set of all indices
10    $d_{max} \leftarrow 0$
11    **for** $j \leftarrow 1 \dots K$ **do**
12       $u_p, v_p \leftarrow \text{argmax}_{(s_p, t_p) \in B} \mathcal{M}[s_p][t_p]$     // pick the max element
13       $d_{max} \leftarrow max(d_{max}, \text{EDGE-SUBMATRIX-DENSITY}(\mathcal{M}, u_p, v_p))$
14       $B \leftarrow B / \{(u_p, v_p)\}$     // remove max element index
15    **return** $d_{max}$     // dense submatrix density

---

**Proposition 7.** *(Proof in Appendix E.2) Time complexity of Algorithm 4 is* $O(|\mathscr{G}| * K * n_r * n_b^2 + |\mathscr{E}| * n_r)$.

**Proposition 8.** *(Proof in Appendix E.2) Memory complexity of Algorithm 4 is* $O(n_r * n_b^2)$.

## 7 Experiments

In this section, we evaluate the performance of our approaches as compared to all baselines discussed in Table 1. We use four real-world datasets: *DARPA* [50] and *ISCX-IDS2012* [51] are popular datasets for graph anomaly detection; [52] surveys more than 30 datasets and recommends to use the newer *CIC-IDS2018* and *CIC-DDoS2019* datasets [53, 54]. Dataset details are discussed in Appendix B. Hyperparameters for the baselines are provided in Appendix H. Appendix F describes the experimental setup and results with some additional parameters are shown in Appendix G. All edge (or graph)-based methods output an anomaly score per edge (or graph), a higher score implying more anomalousness. Similar to baseline papers, we report the Area under the ROC curve (AUC) and the running time. Unless explicitly specified, all experiments including those on the baselines are repeated 5 times and the mean is reported. We aim to answer the following questions:

**Q1. Edge Anomalies:** How accurately do ANOEDGE-G and ANOEDGE-L detect edge anomalies compared to baselines? Are they fast and scalable?

**Q2. Graph Anomalies:** How accurately do ANOGRAPH and ANOGRAPH-K detect graph anomalies i.e. anomalous graph snapshots? Are they fast and scalable?

## 7.1 Edge Anomalies

**Accuracy:** Table 3 shows the AUC of edge anomaly detection baselines, ANOEDGE-G, and ANOEDGE-L. We report a single value for DENSESTREAM and PENminer because these are non-randomized methods. PENminer is unable to finish on the large *CIC-DDoS2019* within 24 hours; thus, that result is not reported. SEDANSPOT uses personalised PageRank to detect anomalies and is not always able to detect anomalous edges occurring in dense block patterns while PENminer is unable to detect structural anomalies. Among the baselines, MIDAS-R is most accurate, however, it performs worse when there is a large number of timestamps as in *ISCX-IDS2012*. Note that ANOEDGE-G and ANOEDGE-L outperform all baselines on all datasets.

Table 3: AUC and Running Time when detecting edge anomalies. Averaged over 5 runs.

| Dataset | DENSESTREAM | SEDANSPOT | MIDAS-R | PENminer | F-FADE | ANOEDGE-G | ANOEDGE-L |
|---|---|---|---|---|---|---|---|
| DARPA | 0.532 | $0.647 \pm 0.006$ | $0.953 \pm 0.002$ | 0.872 | $0.919 \pm 0.005$ | $\mathbf{0.970 \pm 0.001}$ | $0.964 \pm 0.001$ |
|  | 57.7s | 129.1s | 1.4s | 5.21 hrs | 317.8s | 28.7s | 6.1s |
| ISCX-IDS2012 | 0.551 | $0.581 \pm 0.001$ | $0.820 \pm 0.050$ | 0.530 | $0.533 \pm 0.020$ | $0.954 \pm 0.000$ | $\mathbf{0.957 \pm 0.003}$ |
|  | 138.6s | 19.5s | 5.3s | 1.3s | 137.4s | 7.8s | 0.7s |
| CIC-IDS2018 | 0.756 | $0.325 \pm 0.037$ | $0.919 \pm 0.019$ | 0.821 | $0.607 \pm 0.001$ | $\mathbf{0.963 \pm 0.014}$ | $0.927 \pm 0.035$ |
|  | 3.3 hours | 209.6s | 1.1s | 10 hrs | 279.7s | 58.4s | 10.2s |
| CIC-DDoS2019 | 0.263 | $0.567 \pm 0.004$ | $0.983 \pm 0.003$ | — | $0.717 \pm 0.041$ | $0.997 \pm 0.001$ | $\mathbf{0.998 \pm 0.001}$ |
|  | 265.6s | 697.6s | 2.2s | > 24 hrs | 18.7s | 123.3s | 17.8s |

**Running Time:** Table 3 shows the running time (excluding I/O) and real-time performance of ANOEDGE-G and ANOEDGE-L. Since ANOEDGE-L maintains a local dense submatrix, it is faster than ANOEDGE-G. DENSESTREAM maintains dense blocks incrementally for every coming tuple and updates dense subtensors when it meets an updating condition, limiting the detection speed. SEDANSPOT requires several subprocesses (hashing, random-walking, reordering, sampling, etc), PENminer and F-FADE need to actively extract patterns for every graph update, resulting in the large computation time. When there is a large number of timestamps like in *ISCX-IDS2012*, MIDAS-R performs slower than ANOEDGE-L which is the fastest.

**AUC vs Running Time:** Figure 3(a) plots accuracy (AUC) vs. running time (log scale, in seconds, excluding I/O) on the *ISCX-IDS2012* dataset. ANOEDGE-G and ANOEDGE-L achieve much higher accuracy compared to all baselines, while also running significantly fast.
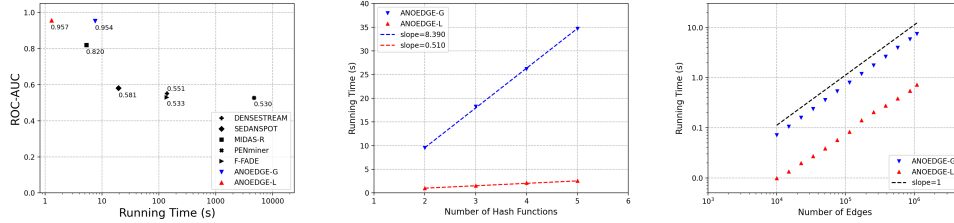


Figure 3: On *ISCX-IDS2012*, (a) AUC vs running time when detecting edge anomalies. (b) Linear scalability with number of hash functions. (c) Linear scalability with number of edges.

**Scalability:** Figures 3(b) and 3(c) plot the running time with increasing number of hash functions and edges respectively, on the *ISCX-IDS2012* dataset. This demonstrates the scalability of ANOEDGE-G and ANOEDGE-L.

## 7.2 Graph Anomalies

**Accuracy:** Table 4 shows the AUC of graph anomaly detection baselines, ANOGRAPH, and ANOGRAPH-K. We report a single value for DENSEALERT and ANOMRANK because these are non-randomized methods. ANOMRANK is not meant for a streaming scenario, therefore the low AUC. DENSEALERT can estimate only one subtensor at a time and SPOTLIGHT uses a randomized approach without any actual search for dense subgraphs. Note that ANOGRAPH and ANOGRAPH-K

outperform all baselines on all datasets while using a simple sketch data structure to incorporate dense subgraph search as opposed to the baselines. We provide results with additional set of parameters in Table 6, Appendix G.

Table 4: AUC and Running Time when detecting graph anomalies. Averaged over 5 runs.

| Dataset | DENSEALERT | SPOTLIGHT | ANOMRANK | **ANOGRAPH** | **ANOGRAPH-K** |
|---|---|---|---|---|---|
| DARPA | 0.833 | $0.728 \pm 0.016$ | 0.754 | $0.835 \pm 0.002$ | $\mathbf{0.839 \pm 0.002}$ |
| | 49.3s | 88.5s | 3.7s | 0.3s | 0.3s |
| ISCX-IDS2012 | 0.906 | $0.872 \pm 0.019$ | 0.194 | $\mathbf{0.950 \pm 0.001}$ | $\mathbf{0.950 \pm 0.001}$ |
| | 6.4s | 21.1s | 5.2s | 0.5s | 0.5s |
| CIC-IDS2018 | 0.950 | $0.835 \pm 0.022$ | 0.783 | $\mathbf{0.957 \pm 0.000}$ | $\mathbf{0.957 \pm 0.000}$ |
| | 67.9s | 149.0s | 7.0s | 0.2s | 0.3s |
| CIC-DDoS2019 | 0.764 | $0.468 \pm 0.048$ | 0.241 | $0.946 \pm 0.002$ | $\mathbf{0.948 \pm 0.002}$ |
| | 1065.0s | 289.7s | 0.2s | 0.4s | 0.4s |

**Running Time:** Table 4 shows the running time (excluding I/O). DENSEALERT has $O(|\mathscr{E}|)$ worse case time complexity (per incoming edge). ANOMRANK needs to compute a global PageRank, which does not scale for stream processing. Note that ANOGRAPH and ANOGRAPH-K run much faster than all baselines.

**AUC vs Running Time:** Figure 4 (a) plots accuracy (AUC) vs. running time (log scale, in seconds, excluding I/O) on the *CIC-DDoS2019* dataset. ANOGRAPH and ANOGRAPH-K achieve much higher accuracy compared to the baselines, while also running significantly faster.

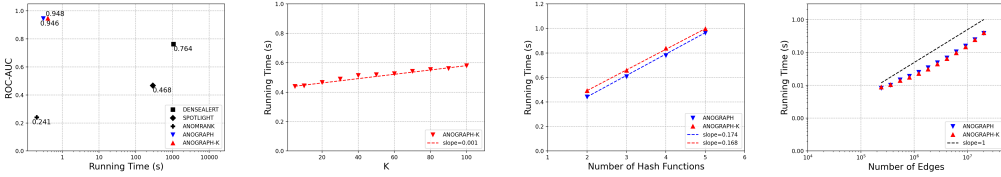

Figure 4: On *CIC-DDoS2019*, (a) AUC vs running time when detecting graph anomalies. (b) ANOGRAPH-K scales linearly with factor $K$. (c) Linear scalability with number of hash functions. (d) Linear scalability with number of edges.

**Scalability:** Figures 4(b), 4(c), and 4(d) plot the running time with increasing factor $K$ (used for top-$K$ in Algorithm 4), number of hash functions and number of edges respectively, on the *CIC-DDoS2019* dataset. This demonstrates the scalability of ANOGRAPH and ANOGRAPH-K.

## 8   Conclusion

In this paper, we extend the CMS data structure to a higher-order sketch to capture complex relations in graph data and to reduce the problem of detecting suspicious dense subgraphs to finding a dense submatrix in constant time. We then propose four sketch-based streaming methods to detect edge and subgraph anomalies in constant time and memory. Furthermore, our approach is the first streaming work that incorporates dense subgraph search to detect graph anomalies in constant memory and time. We also provide a theoretical guarantee on the submatrix density measure and prove the time and space complexities of all methods. Experimental results on four real-world datasets demonstrate our effectiveness as opposed to popular state-of-the-art streaming edge and graph baselines. Future work could consider incorporating node and edge representations, and more general types of data, including tensors.

## References

[1] Kijung Shin, Bryan Hooi, Jisu Kim, and Christos Faloutsos. Densealert: Incremental dense-subtensor detection in tensor streams. *KDD*, 2017.

[2] Dhivya Eswaran, Christos Faloutsos, Sudipto Guha, and Nina Mishra. Spotlight: Detecting anomalies in streaming graphs. In *KDD*, 2018.

[3] Siddharth Bhatia, Bryan Hooi, Minji Yoon, Kijung Shin, and Christos Faloutsos. Midas: Microcluster-based detector of anomalies in edge streams. In *AAAI*, 2020.

[4] Leman Akoglu, Mary McGlohon, and Christos Faloutsos. Oddball: Spotting anomalies in weighted graphs. In *PAKDD*, 2010.

[5] Deepayan Chakrabarti. Autopart: Parameter-free graph partitioning and outlier detection. In *PKDD*, 2004.

[6] Bryan Hooi, Kijung Shin, Hyun Ah Song, Alex Beutel, Neil Shah, and Christos Faloutsos. Graph-based fraud detection in the face of camouflage. *TKDD*, 2017.

[7] Meng Jiang, Peng Cui, Alex Beutel, Christos Faloutsos, and Shiqiang Yang. Catching synchronized behaviors in large networks: A graph mining approach. *TKDD*, 2016.

[8] Jon M Kleinberg. Authoritative sources in a hyperlinked environment. *JACM*, 1999.

[9] Kijung Shin, Tina Eliassi-Rad, and Christos Faloutsos. Patterns and anomalies in k-cores of real-world graphs with applications. *KAIS*, 2018.

[10] Hanghang Tong and Ching-Yung Lin. Non-negative residual matrix factorization with application to graph anomaly detection. In *SDM*, 2011.

[11] Dhivya Eswaran and Christos Faloutsos. Sedanspot: Detecting anomalies in edge streams. In *ICDM*, 2018.

[12] C Belth, X Zheng, and D Koutra. Mining persistent activity in continually evolving networks. In *KDD*, 2020.

[13] Yen-Yu Chang, Pan Li, Rok Sosic, MH Afifi, Marco Schweighauser, and Jure Leskovec. F-fade: Frequency factorization for anomaly detection in edge streams. In *WSDM*, 2021.

[14] Minji Yoon, Bryan Hooi, Kijung Shin, and Christos Faloutsos. Fast and accurate anomaly detection in dynamic graphs with a two-pronged approach. In *KDD*, 2019.

[15] Graham Cormode and Shan Muthukrishnan. An improved data stream summary: the count-min sketch and its applications. *Journal of Algorithms*, 2005.

[16] Jiabao Zhang, Shenghua Liu, Wenjian Yu, Wenjie Feng, and Xueqi Cheng. Eigenpulse: Detecting surges in large streaming graphs with row augmentation. In *PAKDD*, 2019.

[17] Petko Bogdanov, Christos Faloutsos, Misael Mongiovì, Evangelos E Papalexakis, Razvan Ranca, and Ambuj K Singh. Netspot: Spotting significant anomalous regions on dynamic networks. In *SDM*, 2013.

[18] Neil Shah, Alex Beutel, Bryan Hooi, Leman Akoglu, Stephan Gunnemann, Disha Makhija, Mohit Kumar, and Christos Faloutsos. Edgecentric: Anomaly detection in edge-attributed networks. In *ICDMW*, 2016.

[19] Bryan Perozzi and Leman Akoglu. Discovering communities and anomalies in attributed graphs: Interactive visual exploration and summarization. *TKDD*, 2018.

[20] Francesco Bonchi, Ilaria Bordino, Francesco Gullo, and Giovanni Stilo. The importance of unexpectedness: Discovering buzzing stories in anomalous temporal graphs. *Web Intelligence*, 2019.

[21] Francesco Bonchi, Ilaria Bordino, Francesco Gullo, and Giovanni Stilo. Identifying buzzing stories via anomalous temporal subgraph discovery. In *WI*, 2016.

[22] Aleksandar Bojchevski and Stephan Günnemann. Bayesian robust attributed graph clustering: Joint learning of partial anomalies and group structure. In *AAAI*, 2018.

[23] Wenchao Yu, Wei Cheng, C Aggarwal, K Zhang, H Chen, and Wei Wang. Netwalk: A flexible deep embedding approach for anomaly detection in dynamic networks. *KDD*, 2018.

[24] Gyoung S Na, Donghyun Kim, and Hwanjo Yu. Dilof: Effective and memory efficient local outlier detection in data streams. In *KDD*, 2018.

[25] Emaad A Manzoor, Hemank Lamba, and Leman Akoglu. xstream: Outlier detection in feature-evolving data streams. In *KDD*, 2018.

[26] Swee Chuan Tan, Kai Ming Ting, and Tony Fei Liu. Fast anomaly detection for streaming data. In *IJCAI*, 2011.

[27] Dimitrije Jankov, Sourav Sikdar, Rohan Mukherjee, Kia Teymourian, and Chris Jermaine. Real-time high performance anomaly detection over data streams: Grand challenge. *DEBS*, 2017.

[28] Shaofeng Zou, Yingbin Liang, H Vincent Poor, and Xinghua Shi. Nonparametric detection of anomalous data streams. *IEEE Transactions on Signal Processing*, 2017.

[29] Masud Moshtaghi, James C Bezdek, Christopher Leckie, Shanika Karunasekera, and Marimuthu Palaniswami. Evolving fuzzy rules for anomaly detection in data streams. *IEEE Transactions on Fuzzy Systems*, 2015.

[30] Alban Siffer, Pierre-Alain Fouque, Alexandre Termier, Christine Largouet, and C Largouët. Anomaly detection in streams with extreme value theory. *KDD*, 2017.

[31] Maurras Ulbricht Togbe, Mariam Barry, Aliou Boly, Yousra Chabchoub, Raja Chiky, Jacob Montiel, and Vinh-Thuy Tran. Anomaly detection for data streams based on isolation forest using scikit-multiflow. In *ICCSA*, 2020.

[32] Jiabao Zhang, Shenghua Liu, Wenting Hou, Siddharth Bhatia, Hua-Wei Shen, Wenjian Yu, and Xueqi Cheng. Augsplicing: Synchronized behavior detection in streaming tensors. *AAAI*, 2021.

[33] Shirui Pan, Xingquan Zhu, Chengqi Zhang, and S Yu Philip. Graph stream classification using labeled and unlabeled graphs. In *ICDE*, 2013.

[34] Wei Wang, Xiaohong Guan, and Xiangliang Zhang. Processing of massive audit data streams for real-time anomaly intrusion detection. *Computer communications*, 2008.

[35] Aditya Krishna Menon, Gia Vinh Anh Pham, Sanjay Chawla, and Anastasios Viglas. An incremental data-stream sketch using sparse random projections. In *SDM*, 2007.

[36] Peixiang Zhao, Charu C Aggarwal, and Min Wang. gsketch: On query estimation in graph streams. *VLDB*, 2011.

[37] Yang Shi and Animashree Anandkumar. Higher-order count sketch: Dimensionality reduction that retains efficient tensor operations. *DCC*, 2020.

[38] Raghavendra Chalapathy and Sanjay Chawla. Deep learning for anomaly detection: A survey. *ArXiv*, abs/1901.03407, 2019.

[39] Guansong Pang, Chunhua Shen, Longbing Cao, and Anton van den Hengel. Deep learning for anomaly detection: A review. *arXiv preprint arXiv:2007.02500*, 2020.

[40] Leman Akoglu, Hanghang Tong, and Danai Koutra. Graph based anomaly detection and description: A survey. *Data mining and knowledge discovery*, 2015.

[41] Weiren Yu, Charu C Aggarwal, Shuai Ma, and Haixun Wang. On anomalous hotspot discovery in graph streams. In *ICDM*, 2013.

[42] Stephen Ranshous, Steve Harenberg, Kshitij Sharma, and Nagiza F Samatova. A scalable approach for outlier detection in edge streams using sketch-based approximations. In *SDM*, 2016.

[43] Kumar Sricharan and Kamalika Das. Localizing anomalous changes in time-evolving graphs. In *SIGMOD*, 2014.

[44] Jimeng Sun, Dacheng Tao, and Christos Faloutsos. Beyond streams and graphs: dynamic tensor analysis. In *KDD*, 2006.

[45] Alex Beutel, Wanhong Xu, Venkatesan Guruswami, Christopher Palow, and Christos Faloutsos. Copycatch: stopping group attacks by spotting lockstep behavior in social networks. In *WWW*, 2013.

[46] Ehab Abdelhamid, Mustafa Canim, M. Sadoghi, B. Bhattacharjee, Yuan-Chi Chang, and Panos Kalnis. Incremental frequent subgraph mining on large evolving graphs. *TKDE*, 2017.

[47] Lawrence Page, Sergey Brin, Rajeev Motwani, and Terry Winograd. The pagerank citation ranking : Bringing order to the web. In *WWW*, 1999.

[48] Andrew Mcgregor. Graph stream algorithms: a survey. *SIGMOD Record*, 2014.

[49] Samir Khuller and Barna Saha. On finding dense subgraphs. In *ICALP*, 2009.

[50] Richard Lippmann, Robert K Cunningham, David J Fried, Isaac Graf, Kris R Kendall, Seth E Webster, and Marc A Zissman. Results of the darpa 1998 offline intrusion detection evaluation. In *Recent advances in intrusion detection*, 1999.

[51] Ali Shiravi, Hadi Shiravi, Mahbod Tavallaee, and Ali A Ghorbani. Toward developing a systematic approach to generate benchmark datasets for intrusion detection. *computers & security*, 2012.

[52] Markus Ring, Sarah Wunderlich, Deniz Scheuring, Dieter Landes, and Andreas Hotho. A survey of network-based intrusion detection data sets. *Computers & Security*, 2019.

[53] Iman Sharafaldin, Arash Habibi Lashkari, and Ali A Ghorbani. Toward generating a new intrusion detection dataset and intrusion traffic characterization. In *ICISSP*, 2018.

[54] Iman Sharafaldin, Arash Habibi Lashkari, Saqib Hakak, and Ali A Ghorbani. Developing realistic distributed denial of service (ddos) attack dataset and taxonomy. In *ICCST*, 2019.

[55] Random Cut Forest. `https://github.com/aws/random-cut-forest-by-aws`, 2021.

[56] J Lawrence Carter and Mark N Wegman. Universal classes of hash functions. *Journal of computer and system sciences*, 1979.

# Appendix

## A   H-CMS

Algorithm 5 shows the H-CMS operations.

---
**Algorithm 5:** H-CMS Operations

---
1 **Procedure** INITIALIZE H-CMS $(n_r, n_b)$
2    **for** $r \leftarrow 1 \ldots n_r$ **do**
3      $h_r : \mathcal{V} \rightarrow [0, n_b)$              // hash vertex
4      $M_r \rightarrow [0]_{n_b \times n_b}$

1 **Procedure** RESET H-CMS $(n_r, n_b)$
2    **for** $r \leftarrow 1 \ldots n_r$ **do**
3      $\mathcal{M}_r \leftarrow [0]_{n_b \times n_b}$              // reset to zero matrix

1 **Procedure** UPDATE H-CMS $(u, v, w)$
2    **for** $r \leftarrow 1 \ldots n_r$ **do**
3      $\mathcal{M}_r[h_r(u)][h_r(v)] \leftarrow \mathcal{M}_r[h_r(u)][h_r(v)] + w$

1 **Procedure** DECAY H-CMS $(\delta)$
2    **for** $r \leftarrow 1 \ldots n_r$ **do**
3      $\mathcal{M}_r \leftarrow \delta * \mathcal{M}_r$              // decay factor: $\delta$

---

## B   Datasets

Table 5 shows the statistical summary of the datasets. $|E|$ corresponds to the total number of edge records, $|V|$ and $|T|$ are the number of unique nodes and unique timestamps, respectively.

Table 5: Statistics of the datasets.

| Dataset | $|V|$ | $|E|$ | $|T|$ | Edge Anomalies | Graph Anomalies |
|---------|------|------|------|----------------|-----------------|
| DARPA | 25,525 | 4,554,344 | 46,567 | 60.1% | 26.5% |
| ISCX-IDS2012 | 30,917 | 1,097,070 | 165,043 | 4.23% | 3.38% |
| CIC-IDS2018 | 33,176 | 7,948,748 | 38,478 | 7.26% | 11.0% |
| CIC-DDoS2019 | 1,290 | 20,364,525 | 12,224 | 99.7% | 51.4% |

*DARPA* [50] and *ISCX-IDS2012* [51] are popular anomaly detection datasets used by baseline papers to evaluate their algorithms. [52] surveys more than 30 datasets and recommends to use the newer *CIC-IDS2018* [53] and *CIC-DDoS2019* [54] containing modern attack scenarios.

## C   Higher-Order Sketch Proof

**Theorem 1.** *H-CMS has the same estimate guarantees as the original CMS.*

*Proof.* Consider a 3-dimensional H-CMS, with depth $n_r$, where an entity $a \in [1, N]$ is mapped to index $(i, j)$ with two independent hash functions $h' : [1, N] \to [0, b)$ and $h'' : [1, N] \to [0, b)$, i.e., $i = h'(a)$ and $j = h''(a)$. Without loss of generality, the 3-dimensional H-CMS can be converted to a CMS data structure by combining $h'$ and $h''$ in the following way: $h(a) = n_b * h'(a) + h''(a)$, i.e., $h(a) = n_b * i + j$ where $b * i \in [0, n_b^2 - n_b)$ and $j \in [0, n_b]$. Hence, $h(a) \in [0, b^2)$, and $h : [1, N] \to [0, b^2)$ can be a hash function for a CMS data structure with width $n_b^2$ and depth $n_r$. Therefore, the CMS estimate guarantee holds for a 3-dimensional H-CMS data structure. A higher dimensional H-CMS can be reduced to a CMS data structure in a similar manner. $\square$

## D   Edge Anomalies Proofs

### D.1   Proofs: ANOEDGE-G

**Proposition 1.** *Time complexity of Algorithm 1 is $O(|\mathscr{E}| * n_r * n_b^2)$.*

*Proof.* Procedure EDGE-SUBMATRIX-DENSITY removes rows (or columns) iteratively, and the total number of rows and columns that can be removed is $n_b + n_b - 2$. In each iteration, the approach performs the following three operations: (a) pick the row with minimum row-sum; (b) pick the column with minimum column-sum; (c) calculate density. We keep $n_b$-sized arrays for flagging removed rows (or columns), and for maintaining row-sums (or column-sums). Operations (a) and (b) take maximum $n_b$ steps to pick and flag the row with minimum row-sum (or column-sum). Updating the column-sums (or rows-sums) based on the picked row (or column) again takes maximum $n_b$ steps. Time complexity of (a) and (b) is therefore $O(n_b)$. Density is directly calculated based on subtracting the removed row-sum (or column-sum) and reducing the row-count (or column-count) from the earlier density value. Row-count and column-count are kept as separate variables. Therefore, the time complexity of the density calculation step is $O(1)$. Total time complexity of procedure EDGE-SUBMATRIX-DENSITY is $O((n_b + n_b - 2) * (n_b + n_b + 1)) = O(n_b^2)$.

Time complexity to initialize and decay the H-CMS data structure is $O(n_r * n_b^2)$. Temporal decay operation is applied whenever the timestamp changes, and not for every received edge. Update counts operation updates a matrix element value ($O(1)$ operation) for $n_r$ matrices, and the time complexity of this step is $O(n_r)$. Anomaly score for each edge is based on the submatrix density computation procedure which is $O(n_b^2)$; the time complexity of $n_r$ matrices becomes $O(n_r * n_b^2)$. Therefore, the total time complexity of Algorithm 1 is $O(|\mathscr{E}| * (n_r + n_r * n_b^2)) = O(|\mathscr{E}| * n_r * n_b^2)$. $\square$

**Proposition 2.** *Memory complexity of Algorithm 1 is $O(n_r * n_b^2)$.*

*Proof.* For procedure EDGE-SUBMATRIX-DENSITY, we keep an $n_b$-sized arrays to flag rows and columns that are part of the current submatrix, and to maintain row-sums and column-sums. Total memory complexity of EDGE-SUBMATRIX-DENSITY procedure is $O(4 * n_b) = O(n_b)$.

Memory complexity of H-CMS data structure is $O(n_r * n_b^2)$. Dense submatrix search and density computation procedure require $O(n_b)$ memory. For $n_r$ matrices, this becomes $O(n_r * n_b)$. Therefore, the total memory complexity of Algorithm 1 is $O(n_r * n_b^2 + n_r * n_b) = O(n_r * n_b^2)$. $\square$

### D.2   Proofs: ANOEDGE-L

**Proposition 3.** *Time complexity of Algorithm 2 is $O(n_r * n_b^2 + |\mathscr{E}| * n_r * n_b)$.*

14

*Proof.* As shown in Proposition 1, the time complexity of H-CMS is $O(n_r * n_b^2)$ and update operation is $O(n_r)$. Current submatrix $(S_{cur}, T_{cur})$ is updated based on *expand* and *condense* submatrix operations. (a) We keep an $n_b$-sized array to flag the current submatrix rows (or column), and also to maintain row-sums (or column-sums). Expand submatrix operation depends on the elements from row $h(u)$ and column $h(v)$, and the density is calculated by considering these elements, thus requiring maximum $n_b$ steps. Upon addition of the row (or column), the dependent column-sums (or row-sums) are also updated taking maximum $n_b$ steps. Time complexity of expand operation is therefore $O(n_b)$. (b) Condense submatrix operation removes rows and columns iteratively. A row (or column) elimination is performed by selecting the row (or column) with minimum row-sum (or column-sum) in $O(n_b)$ time. Removed row (or column) affects the dependent column-sums (or row-sums) and are updated in $O(n_b)$ time. Time complexity of a row (or column) removal is therefore $O(n_b)$. Condense submatrix removes rows (or columns) that were once added by the expand submatrix operation which in worse case is $O|\mathscr{E}|$.

Expand and condense submatrix operations are performed for $n_r$ matrices. Likelihood score calculation depends on elements from row $h(u)$ and column $h(v)$, and takes $O(n_r * n_b)$ time for $n_r$ matrices. Therefore, the total time complexity of Algorithm 2 is $O(n_r * n_b^2 + |\mathscr{E}| * n_r + |\mathscr{E}| * n_r * n_b + |\mathscr{E}| * n_r * n_b + |\mathscr{E}| * n_r * n_b) = O(n_r * n_b^2 + |\mathscr{E}| * n_r * n_b)$. $\square$

**Proposition 4.** *Memory complexity of Algorithm 2 is $O(n_r * n_b^2)$.*

*Proof.* Memory complexity of the H-CMS data structure is $O(n_r * n_b^2)$. To keep current submatrix information, we utilize $n_b$-sized arrays similar to Proposition 2. For $n_r$ matrices, submatrix information requires $O(n_r * n_b)$ memory. Hence, total memory complexity of Algorithm 2 is $O(n_r * n_b^2 + n_r * n_b) = O(n_r * n_b^2)$. $\square$

# E  Graph Anomalies-Proofs

## E.1  Proofs: ANOGRAPH

**Lemma 1.** *Let $S^*$ and $T^*$ be the optimum densest sub-matrix solution of $\mathcal{M}$ with density $\mathcal{D}(\mathcal{M}, S^*, T^*) = d_{opt}$. Then $\forall u \in S^*$ and $\forall v \in T^*$,*

$$\mathcal{R}(\mathcal{M}, u, T^*) \geq \tau_{S^*}; \quad \mathcal{C}(\mathcal{M}, S^*, v) \geq \tau_{T^*} \tag{3}$$

*where:* $\tau_{S^*} = \mathcal{E}(\mathcal{M}, S^*, T^*)\left(1 - \sqrt{1 - \frac{1}{|S^*|}}\right),$

$\tau_{T^*} = \mathcal{E}(\mathcal{M}, S^*, T^*)\left(1 - \sqrt{1 - \frac{1}{|T^*|}}\right)$

*Proof.* Leveraging the proof from [49], let's assume that $\exists u \in S^*$ with $\mathcal{R}(\mathcal{M}, u, T^*) < \tau_{S^*}$. Density of submatrix after removing $u = \frac{\mathcal{E}(\mathcal{M}, S^*, T^*) - \mathcal{R}(\mathcal{M}, u, T^*)}{\sqrt{(|S^* - 1|)|T^*|}}$ which is greater than $\frac{\mathcal{E}(\mathcal{M}, S^*, T^*) - \tau_{S^*}}{\sqrt{(|S^* - 1|)|T^*|}} = d_{opt}$, and that is not possible. Hence, $\mathcal{R}(\mathcal{M}, u, T^*) \geq \tau_{S^*}$. $\mathcal{C}(\mathcal{M}, S^*, v) \geq \tau_{T^*}$ can be proved in a similar manner. $\square$

**Theorem 2.** *Algorithm 3 achieves a 2-approximation guarantee for the densest submatrix problem.*

*Proof.* Leveraging the proof from [49], we greedily remove the row (or column) with minimum row-sum (or column-sum). At some iteration of the greedy process, $\forall u \in S_{cur}; \forall v \in T_{cur}$, $\mathcal{R}(\mathcal{M}, u, T_{cur}) \geq \tau_{S^*}$ and $\mathcal{C}(\mathcal{M}, S_{cur}, v) \geq \tau_{T^*}$. Therefore, $\mathcal{E}(\mathcal{M}, S_{cur}, T_{cur}) \geq |S_{cur}|\tau_{S^*}$ and $\mathcal{E}(\mathcal{M}, S_{cur}, T_{cur}) \geq |T_{cur}|\tau_{T^*}$. This implies that the density $\mathcal{D}(\mathcal{M}, S_{cur}, T_{cur}) \geq \sqrt{\frac{|S_{cur}|\tau_{S^*}|T_{cur}|\tau_{T^*}}{|S_{cur}||T_{cur}|}} = \sqrt{\tau_{S^*}\tau_{T^*}}$. Putting values of $\tau_{S^*}$ and $\tau_{T^*}$ from Lemma 1, and setting $|S^*| = \frac{1}{\sin^2 \alpha}$, $|T^*| = \frac{1}{\sin^2 \beta}$, we get $\mathcal{D}(\mathcal{M}, S_{cur}, T_{cur}) \geq \frac{\mathcal{E}(\mathcal{M}, S^*, T^*)}{\sqrt{|S^*||T^*|}} \frac{\sqrt{(1 - \cos \alpha)(1 - \cos \beta)}}{\sin \alpha \sin \beta} \geq \frac{d_{opt}}{2 \cos \frac{\alpha}{2} \cos \frac{\beta}{2}} \geq \frac{d_{opt}}{2}$. $\square$

**Proposition 5.** *Time complexity of Algorithm 3 is $O(|\mathscr{G}| * n_r * n_b^2 + |\mathscr{E}| * n_r)$.*

*Proof.* Procedure ANOGRAPH-DENSITY iteratively removes row (or column) with minimum row-sum (or column-sum). Maximum number of rows and columns that can be removed is $n_b + n_b - 2$. We keep $n_b$-sized arrays to store the current submatrix rows and columns, and row-sums and column-sums. At each iteration, selecting the row (or column) with minimum row-sum (or column-sum) takes $O(n_b)$ time, and updating the dependent row-sums (or column-sums) also $O(n_b)$ time. Density is calculated in $O(n_b)$ time based on the current submatrix row-sum and column-sum. Each iteration takes $O(n_b + n_b + n_b) = O(n_b)$ time. Hence, the total time complexity of ANOGRAPH-DENSITY procedure is $O((n_b + n_b - 2) * n_b) = O(n_b^2)$.

Initializing the H-CMS data structure takes $O(n_r * n_b^2)$ time. When a graph arrives, ANOGRAPH: (a) resets counts that take $O(n_r * n_b^2)$ time; (b) updates counts taking $O(1)$ time for every edge update; (c) computes submatrix density that follows from procedure ANOGRAPH-DENSITY and takes $O(n_b^2)$ time. Each of these operations is applied for $n_r$ matrices. Therefore, the total time complexity of Algorithm 3 is $O(n_r * n_b^2 + |\mathscr{G}| * n_r * n_b^2 + |\mathscr{E}| * n_r + |\mathscr{G}| * n_r * n_b^2) = O(|\mathscr{G}| * n_r * n_b^2 + |\mathscr{E}| * n_r)$, where $|\mathscr{E}|$ is the total number of edges over graphs $\mathscr{G}$. □

**Proposition 6.** *Memory complexity of Algorithm 3 is $O(n_r * n_b^2)$.*

*Proof.* For procedure ANOGRAPH-DENSITY, we keep $n_b$-sized array to flag rows and columns that are part of the current submatrix, and to maintain row-sums and column-sums. Hence, memory complexity of ANOGRAPH-DENSITY procedure is $O(4 * n_b) = O(n_b)$.

H-CMS data structure requires $O(n_r * n_b^2)$ memory. Density computation relies on ANOGRAPH-DENSITY procedure, and takes $O(n_b)$ memory. Therefore, the total memory complexity of Algorithm 3 is $O(n_r * n_b^2)$. □

### E.2  Proofs: ANOGRAPH-K

**Proposition 7.** *Time complexity of Algorithm 4 is $O(|\mathscr{G}| * K * n_r * n_b^2 + |\mathscr{E}| * n_r)$.*

*Proof.* Relevant operations in Procedure ANOGRAPH-K-DENSITY directly follow from EDGE-SUBMATRIX-DENSITY procedure, which has $O(n_b^2)$ time complexity. EDGE-SUBMATRIX-DENSITY procedure is called $K$ times, therefore, the total time complexity of ANOGRAPH-K-DENSITY procedure is $O(K * n_b^2)$.

For Algorithm 4, we initialize an H-CMS data structure that takes $O(n_r * n_b^2)$ time. When a graph arrives, ANOGRAPH-K: (a) resets counts that take $O(n_r * n_b^2)$ time; (b) updates counts taking $O(1)$ time for every edge update; (c) computes submatrix density that follows from procedure ANOGRAPH-K-DENSITY and takes $O(K * n_b^2)$ time. Each of these operations is applied for $n_r$ matrices. Therefore, the total time complexity of Algorithm 4 is $O(n_r * n_b^2 + |\mathscr{G}| * K * n_r * n_b^2 + |\mathscr{E}| * n_r + |\mathscr{G}| * n_r * n_b^2) = O(|\mathscr{G}| * K * n_r * n_b^2 + |\mathscr{E}| * n_r)$, where $|\mathscr{E}|$ is the total number of edges over graphs $\mathscr{G}$. □

**Proposition 8.** *Memory complexity of Algorithm 4 is $O(n_r * n_b^2)$.*

*Proof.* The density of $K$ submatrices is computed independently, and the memory complexity of Algorithm procedure ANOGRAPH-K-DENSITY is the same as the memory complexity of EDGE-SUBMATRIX-DENSITY procedure i.e. $O(n_b)$.

Maintaining the H-CMS data structure requires $O(n_r * n_b^2)$ memory. Density computation relies on ANOGRAPH-K-DENSITY procedure, and it requires $O(n_b)$ memory. Therefore, the total memory complexity of Algorithm 4 is $O(n_r * n_b^2)$. □

## F  Experimental Setup

All experiments are carried out on a $2.4GHz$ Intel Core $i9$ processor, $32GB$ RAM, running OS $X$ 10.15.3. For our approach, we keep $n_r = 2$ and temporal decay factor $\delta = 0.9$. $n_b = 32$ to have a fair comparison to MIDAS which uses $n_b{}^2 = 1024$ buckets. We keep $K = 5$ for Algorithm 4. AUC for graph anomalies is shown with edge thresholds as 50 for *DARPA* and 100 for other datasets. Time window is taken as 30 minutes for *DARPA* and 60 minutes for other datasets.

# G  Additional Results

Table 6 shows the performance of ANOGRAPH and ANOGRAPH-K for different time windows and edge thresholds. The edge threshold is varied in such a way that a sufficient number of anomalies are present within the time window. ANOGRAPH and ANOGRAPH-K have performance similar to that in Table 4.

Table 6: AUC when detecting graph anomalies.

| Dataset | Time Window | Edge Threshold | ANOGRAPH | ANOGRAPH-K |
|---|---|---|---|---|
| DARPA | 15 | 25 | $0.835 \pm 0.001$ | $0.838 \pm 0.001$ |
| | 30 | 50 | $0.835 \pm 0.002$ | $0.839 \pm 0.002$ |
| | 60 | 50 | $0.747 \pm 0.002$ | $0.748 \pm 0.001$ |
| | 60 | 100 | $0.823 \pm 0.000$ | $0.825 \pm 0.001$ |
| ISCX-IDS2012 | 15 | 25 | $0.945 \pm 0.001$ | $0.945 \pm 0.000$ |
| | 30 | 50 | $0.949 \pm 0.001$ | $0.948 \pm 0.000$ |
| | 60 | 50 | $0.935 \pm 0.002$ | $0.933 \pm 0.002$ |
| | 60 | 100 | $0.950 \pm 0.001$ | $0.950 \pm 0.001$ |
| CIC-IDS2018 | 15 | 25 | $0.945 \pm 0.004$ | $0.947 \pm 0.006$ |
| | 30 | 50 | $0.959 \pm 0.000$ | $0.959 \pm 0.001$ |
| | 60 | 50 | $0.920 \pm 0.001$ | $0.920 \pm 0.001$ |
| | 60 | 100 | $0.957 \pm 0.000$ | $0.957 \pm 0.000$ |
| CIC-DDoS2019 | 15 | 25 | $0.864 \pm 0.002$ | $0.863 \pm 0.003$ |
| | 30 | 50 | $0.861 \pm 0.003$ | $0.861 \pm 0.003$ |
| | 60 | 50 | $0.824 \pm 0.004$ | $0.825 \pm 0.005$ |
| | 60 | 100 | $0.946 \pm 0.002$ | $0.948 \pm 0.002$ |

# H  Baselines

We use open-source implementations of DENSESTREAM [1] (Java), SEDANSPOT [11] (C++), MIDAS-R [3] (C++), PENminer [12] (Python), F-FADE [13] (Python), DENSEALERT [1] (Java), and ANOMRANK [14] (C++) provided by the authors, following parameter settings as suggested in the original paper. For SPOTLIGHT [2], we used open-sourced implementations of Random Cut Forest [55] and Carter Wegman hashing [56].

## H.1  Edge Anomalies

1. SEDANSPOT:
    - `sample_size` $= 10000$
    - `num_walk` $= 50$
    - `restart_prob` $0.15$

2. MIDAS: The size of CMSs is 2 rows by 1024 columns for all the tests. For MIDAS-R, the decay factor $\alpha = 0.6$.

3. PENminer:
    - `ws` $= 1$
    - `ms` $= 1$
    - `view` $=$ `id`
    - `alpha` $= 1$
    - `beta` $= 1$
    - `gamma` $= 1$

4. DENSESTREAM: We keep default parameters, i.e., order $= 3$.

5. F-FADE:
   - `embedding_size` $= 200$
   - `W_upd` $= 720$
   - `T_th` $= 120$
   - `alpha` $= 0.999$
   - `M` $= 100$

   For `t_setup`, we always use the timestamp value at the $10^{th}$ percentile of the dataset.

## H.2 Graph Anomalies

1. SPOTLIGHT:
   - `K` $= 50$
   - `p` $= 0.2$
   - `q` $= 0.2$

2. DENSEALERT: We keep default parameters, i.e., order $= 3$ and window=60.

3. ANOMRANK: We keep default parameters, i.e., damping factor c $= 0.5$, and L1 changes of node score vectors threshold epsilon $= 10^{-3}$. We keep $1/4^{th}$ number of graphs for initializing mean/variance as mentioned in the respective paper.